Alterations in the polysialylated neural cell adhesion molecule and retinal ganglion cell density in mice with diabetic retinopathy

Natalia Lobanovskaya, Monika Jürgenson, Anu Aonurm-Helm, Alexander Zharkovsky

Department of Pharmacology, Centre of Excellence for Translational Medicine, University of Tartu, Tartu 50411, Estonia

Correspondence to: Natalia Lobanovskaya. Department of Pharmacology, Centre of Excellence for Translational Medicine, University of Tartu, Ravila 19, Tartu 50411, Estonia. natalia.lobanovskaya@gmail.com

Abstract

● **AIM:** To investigate the impact of polysialylated neural cell adhesion molecule (PSA-NCAM) on the survival of retinal ganglion cells (RGCs) in the experimentally induced diabetes in mice.

● **METHODS:** Diabetes was induced in 2.5 months old Swiss Webster mice by intraperitoneal injection of streptozotocin (STZ, 90 mg/kg) once daily for two consecutive days. Examination of the proteins of interest in the retinas from diabetic mice at 2mo after diabetes induction was performed using immunohistochemistry and Western blot analysis. RGCs were counted in the wholemounted retinas, and Brn3a marker was used.

● **RESULTS:** Examination of retinas from diabetic mice at 2mo after diabetes induction revealed a considerable reduction in RGC density. Our experiments also demonstrated a redistribution of PSA-NCAM in the retina of diabetic animals. PSA-NCAM immunoreactivity was diminished in the inner part of the retina where RGCs were located. In contrast, an enhanced PSA-NCAM immunoreactivity was detected in the outer layers of the retina. PSA-NCAM signal was co-localized with glial fibrillary acidic protein immunoreactivity in the Müller cell branches. Previous studies have shown that matrix metalloproteinase-9 (MMP-9) is responsible for the reduction in PSA-NCAM levels in neuronal cells. The reduced levels of PSA-NCAM in inner layers (nerve fiber layer, ganglion cell layer) were accompanied by the increased expression of MMP-9. In contrast, in the outer retinal layers, the expression of MMP-9 was much less pronounced.

● **CONCLUSION:** MMP-9 induces PSA-NCAM shedding in the inner part of the retina and the decreased level of PSA-

NCAM in the inner part of the retina might be, at least in part, responsible for the loss of RGCs in diabetic mice.

INTRODUCTION

Diabetic retinopathy (DR) is a common complication of diabetes. It can cause blindness in humans if left undiagnosed and untreated. Proliferative DR leads to intraretinal and intravitreal haemorrhages, glial cell proliferation and neovascularization, and tractional retinal detachment. Effects of diabetes on the retina have been studied in rodent models[1-3]. In animals, the most frequently used model is the streptozotocin (STZ) diabetic model[4-5]. STZ is particularly toxic to the insulin-producing beta-cells of the pancreas in mammals and, depending on the dose, it can induce either Type 1 or Type 2 diabetes[6]. It is well established that DR damages retinal vasculature in rodents[7-9]. It has been shown that retinal ganglion cells (RGCs) are affected in both human and experimental diabetes. In diabetic rats and mice, RGCs undergo apoptosis and Müller cells are activated[3,10-11]. However, some studies have failed to detect the degeneration of the RGCs in diabetic mice[12]. This discrepancy is probably due to the different sensitivity of mice and rats to STZ[13].

Neural cell adhesion molecule (NCAM) is a cell surface glycoprotein of the immunoglobulin superfamily of adhesion molecules. Polysialic acid (PSA) comprises alpha 2-8-linked sialic acid, and it is almost exclusively found attached to NCAM in mammals. In the central nervous system (CNS), it has been established that polysialylated neural cell adhesion molecule (PSA-NCAM) plays a role in synaptic plasticity, axon growth and migration, mediates cell interactions, and promotes the survival of neurons during development and cell regeneration. During embryogenesis, PSA is highly enriched on NCAM in many regions of the CNS but levels of polysialylated NCAM decrease soon after birth[14-15]. However,

it persists in the mature brain in the regions where ongoing plasticity and neurogenesis occur[16].

During development, NCAM is highly sialylated on the surface of cells in all retinal layers[17]. In adulthood, PSA-NCAM is expressed abundantly by astrocytes and endfeet of Müller cells in mice[17-18]. Expression of NCAM by astrocytes was found in the human optic nerve head[19]. Human retinal pigment epithelial cells demonstrated expression of NCAM[20]. However, the roles of PSA-NCAM in the human retina are still unclear. Müller cells refer to radial cell glia, and they provide architectural support stretching radially across the thickness of the retina. In the adult retina, astrocyte cell bodies and processes are almost exclusively confined to the nerve fiber layer (NFL) and ganglion cell layer (GCL) of the retina[21-22]. The soma of ganglion cells is covered by a close-fitting sheath formed by Müller cells. Intraretinal length of RGC axons is partly vested by both astrocytes and Müller cells[23], and PSA-NCAM stays in close proximity to the RGC layer in adulthood. Glial fibrillary acidic protein (GFAP) is widely used as a marker to detect astrocytes and Müller cells. Removal of PSA from NCAM enhanced RGC degeneration in the normal retina and following optic nerve transection or administration of the neurotoxin kainic acid[24]. Mice with constitutive deficiency of NCAM demonstrated earlier RGC loss following optic nerve cut[25]. It was shown that PSA-NCAM can be cleaved extracellularly by matrix metalloproteinase-9 (MMP-9)[26]. MMPs are zinc-containing endopeptidase. These enzymes are capable of degrading all kinds of extracellular matrix proteins. It was demonstrated in the several studies that MMP-9 is the most abundantly present in the retina during different pathological conditions including DR. Thus, the aim of this study was to explore whether or not DR is associated with alterations in PSA-NCAM expression/distribution in the adult mouse retina and if it influences RGC survival.
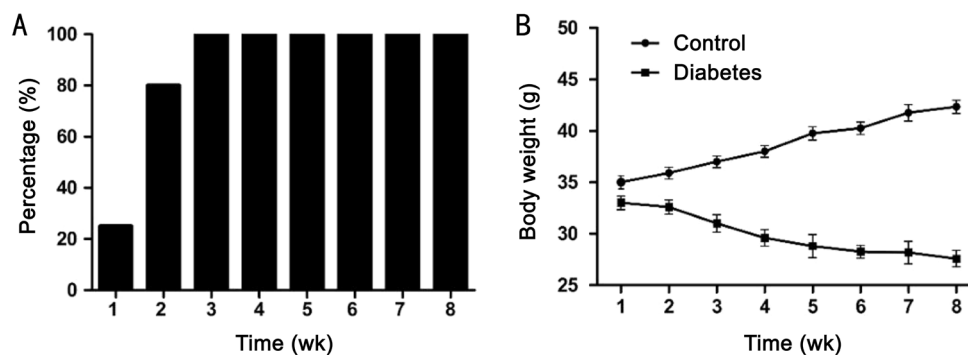
MATERIALS AND METHODS

Materials All experiments were undertaken in agreement with the guidelines established in the Principles of Laboratory Animal Care (Directive 2010/63/EU). All experimental procedures conformed to local guidelines on the ethical use of animals and were conducted by persons who hold a proper licence. The animals were handled in accordance with the ARVO Statement for the Use of Animals in Ophthalmic and Vision Research. Twenty-four male Swiss Webster mice at 2-2.5 month of age were group-housed (four mice per cage) with a 12h light/dark cycle. Half of the animals were made diabetic by intraperitoneal injection of 90 mg/kg STZ (Sigma-Aldrich, St Louis, MO, USA). STZ was freshly dissolved in the sodium citrate buffer, pH 4.5 and injected once daily for two consecutive days[27]. Control mice were injected with vehicle only. Mice were screened for diabetes beginning at one week after the last injection of STZ by measuring glucose levels in a drop of blood obtained from the tail (glucometer

GLUCOCARD™ X-METER). Insulin was not administered to the animals. Blood glucose levels and weight of the animals were measured once weekly. Mice were euthanized at two months after the onset of diabetes.

Retinal Ganglion Cell Density Analyses RGC staining was performed in wholemount retinas using a Brn3a marker[28-29] as it was done previously[24]. To evaluate the density of Brn3a-positive cells a stereology system comprising an Olympus BX-51 microscope and Visiopharm Integrator System (Version 3.6.5.0, Denmark) was applied. Forty visual fields (625 μm^2) were randomly sampled for each retina. The average density of Brn3a-positive cells in one retina was quantified per mm^2 for each animal in control (n=6) and diabetic (n=6) groups.

Microglial Cell Density Analysis Microglial cell staining was done on the retinal sections using an Iba1 marker[30]. Mice were perfused and eye cups were sectioned at 18 μm making use of a cryostat (Leica Biosystems CM1850, Germany) as it was described before[24]. Endogenous peroxidase activity was blocked with 3% H$_2$O$_2$. Then retinal sections were incubated with primary goat anti-Iba1 antibody (Abcam, USA), diluted 1:100 in blocking solution containing 3% rabbit serum overnight, followed by incubation with biotinylated rabbit anti-goat IgG antibody (Vector Laboratories, USA), diluted 1:200 in phosphate buffer solution (PBS). Peroxidase method (Vectastain ABC kit and Peroxidase substrate kit DAB, Vector Laboratories, USA) was employed for Iba1-positive cell visualization. The sections were air-dried and mounting medium (Roti-Histokitt II, Germany) was laid on. To quantify the density of Iba1-positive cells a stereology system comprising an Olympus BX-51 microscope and Visiopharm Integrator System (Version 3.6.5.0, Denmark) was used. Five visual fields (0.04 mm^2) were randomly sampled for each section (n=3 per animal). The average density of Iba1-positive cells was calculated per mm^2 for each animal in control (n=6) and diabetic (n=6) groups.

Immunoblotting Analysis Tissue preparation, supernatants resolving and proteins transferring onto membranes was done as previously described[24]. Afterwards the membranes were incubated with Odyssey Blocking Buffer (LI-COR Biotechnology, USA). Primary antibodies: mouse anti-PSA-NCAM antibody (1:1000; IgM, clone: 2-2B; AbCys, France) or mouse anti-GFAP antibody (1:1000; IgG, clone 2-A-5, Chemicon, UK) or rabbit anti-β-actin antibody (1:5000; Sigma, St. Louis, USA) were applied overnight. Then the membranes were incubated with the secondary antibodies: biotinylated goat anti-mouse IgM antibody (1:2000; Vector Laboratories, Inc. USA), IR Dye 680 LT Streptavidin (1:10 000; LI-COR, Germany) or goat anti-mouse IR Dye 680 LT antibody (1:10 000; LI-COR, Germany) or goat anti-rabbit IR-Dye 800 CW antibody (1:10 000; LI-COR, USA). The membranes were analysed with Odyssey CLx Infrared Imaging System (USA). The proteins' optical density ratios were then computed.

Figure 1 The development of diabetes after STZ administration in mice A: Percentage of animals with glucose levels 33 mmol/L or higher; B: Body weight (g). n=12 in each group; the data of body weight are given as mean±SEM.

PSA-NCAM, GFAP, MMP-9 Immunohistochemistry For PSA-NCAM, GFAP, and MMP-9 immunohistochemistry, three sections per animal for each protein were chosen randomly from control (n=6) and diabetic (n=6) groups. Endogenous peroxidase activity was blocked with 3% H_2O_2. Next the sections were incubated with primary antibodies: mouse anti-PSA-NCAM antibody (1:400; IgM, clone: 2-2B; AbCys, France) or rabbit anti-GFAP antibody (1:1000; Dako, Denmark) or goat anti-MMP-9 antibody (1:500; Abcam, USA) followed by incubation with appropriate biotinylated anti-mouse, anti-rabbit or anti-goat antibodies (1:200; IgM, Vector Laboratories, Inc., USA). PSA-NCAM, GFAP and MMP-9 proteins were visualized using the peroxidase method (Vectastain ABC kit and Peroxidase substrate kit DAB, Vector Laboratories, USA). The sections were air-dried and mounting medium (Roti-Histokitt II, Germany) was laid on. Immunoreactivity for PSA-NCAM, GFAP and MMP-9 were observed using an Olympus BX-51 microscope.

For immunofluorescent co-expression of PSA-NCAM and astrocyte marker (GFAP), sections were incubated with a mixture of mouse anti-PSA-NCAM antibody (1:400; IgM, clone: 2-2B; AbCys, France) and rabbit anti-GFAP antibody (1:500; Dako, Denmark). Secondary antibodies: Alexa Fluor 594 goat anti-mouse IgM (1:500; Invitrogen Molecular probes, USA) and Alexa Fluor 488 goat anti-rabbit IgG (H+L) (1:500; Invitrogen Molecular probes, USA) were used. Fluorescence signals were detected with a confocal microscope LSM 510 (Zeiss, Germany) and further analysed for the co-localization of PSA-NCAM signal with GFAP. DP55561-10, 561 nm and Argon/2 458, 477, 488, 514 nm lasers were used.

Analysis of PSA-NCAM and MMP-9 Immunoreactivity Quantification of intensity of PSA-NCAM and MMP-9 immunoreactivity in the retina sections was evaluated in the following areas: NFL and GCL, inner plexiform layer (IPL) and inner nuclear layer (INL), outer plexiform layer (OPL) and outer nuclear layer (ONL). Mean gray value (MGV) of immunopositive profiles was measured using ImageJ software. Images were grey-scaled to 8-bit, and a grid overlay was applied. MGV in the crosses of the grid was measured
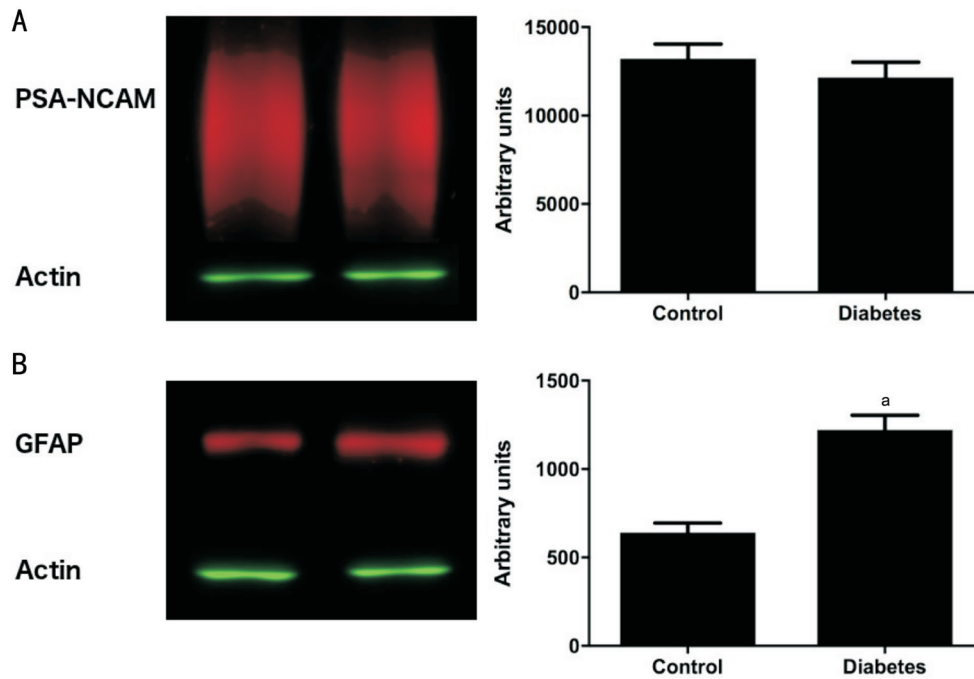
in each area of interest for immunopositive profile and in the background. MGV of 8-bit images in ImageJ reflects an average intensity of pixels over a range of 0 (black) to 255 (white). MGV of each area was then expressed as a ratio, which was called the immunoreactivity index (IR index)[31-32]. The IR index is: IR index=$(1-I_{cell}/I_{bg})\times100$, where I_{cell} is the MGV of the immunopositive profile, I_{bg} is the MGV of the background in that field. The IR index increases with immunostaining intensity.

Statistical Analysis The results are expressed as the mean±SEM. Statistical analyses were performed using Mann-Whitney (non-parametric) or Student's t-test (parametric), where appropriate. Two-way ANOVA for repeated measures was used to assess the changes in the body weight.
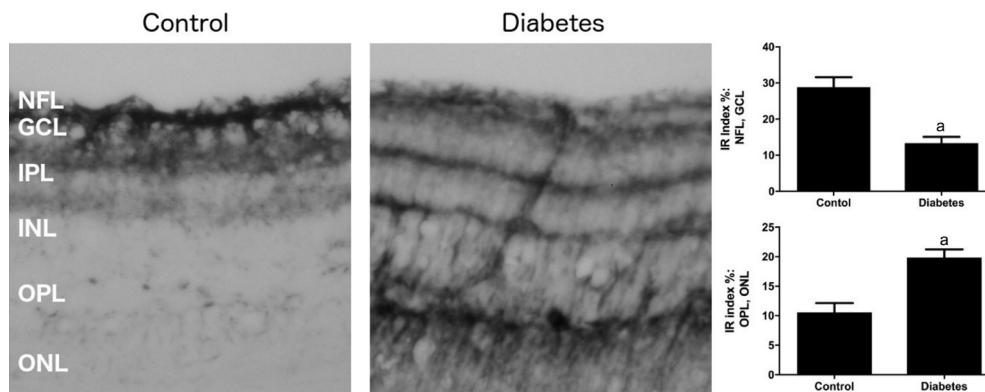
RESULTS

Development of Streptozotocin Diabetes in Mice The administration of STZ resulted in the rapid and stable rise in glucose levels. All animals demonstrated elevated blood glucose levels (P<0.05, Student's t-test) already at the end of the first week 28±1.8 mmol/L (n=12). At the end of the second week 80% of mice and at the third week all animals (n=12) demonstrated glucose levels 33 mmol/L (the highest detection level by the glucometer) and were considered to be diabetic (Figure 1). In control animals, the glucose levels were 8.9± 1.2 mmol/L (n=12). At two months after the onset of diabetes, treated mice weighed significantly less than control mice (Figure 1). For the body weight changes, a two-way ANOVA demonstrated a significant effect of treatment ($F_{1,84}$=162; P<0.0001), a significant effect of time ($F_{5,84}$=23.93; P<0.0001) and a significant effect of interaction ($F_{5,84}$=9.419; P<0.0001).

Changes in the Density of Retinal Ganglion Cells and Microglial Cells in Diabetic Mice To examine whether diabetes affects the density of RGCs, we performed Brn3a immunohistochemistry in wholemount retinas of diabetic and control animals. Brn3a has been shown to be specifically expressed by RGCs in mice and can be used as an efficient marker to identify and quantify RGCs[28-29]. Our experiments demonstrated significantly lower density of RGCs in diabetic mice at two months after onset of diabetes compared with

Figure 2 Western blot analysis demonstrating PSA-NCAM protein levels (A) and GFAP levels (B) in control and diabetic retinas The data are expressed as the mean±SEM. [a]$P<0.0022$ (Mann-Whitney U test).

Figure 3 Representative microphotographs of PSA-NCAM immunoreactivity in retinal sections of control and diabetic mice Magnification ×200. IR: Immunoreactivity; NFL: Nerve fiber layer; GCL: Ganglion cell layer; IPL: Inner plexiform layer; INL: Inner nuclear layer; OPL: Outer plexiform layer; ONL: Outer nuclear layer. The data are expressed as the mean±SEM. [a]$P<0.0022$ (Mann-Whitney U test).

controls (Table 1). At this time point, a reduction in density of RGCs by approximately 19% was observed in diabetic animals. Our experiments also demonstrated an increased density and hypertrophy of microglial (Iba1-positive) cells in diabetic retina (Table 1), which suggests the existence of inflammation in DR.

Redistribution of PSA-NCAM Immunohistochemical Signal in Diabetic Mice Western blot did not reveal any changes in the total levels of PSA-NCAM protein in diabetic retina compared with controls (Figure 2A). Note: PSA-NCAM appears on the blot as a smear (180-220 kDa) due to the different size of PSA residues.
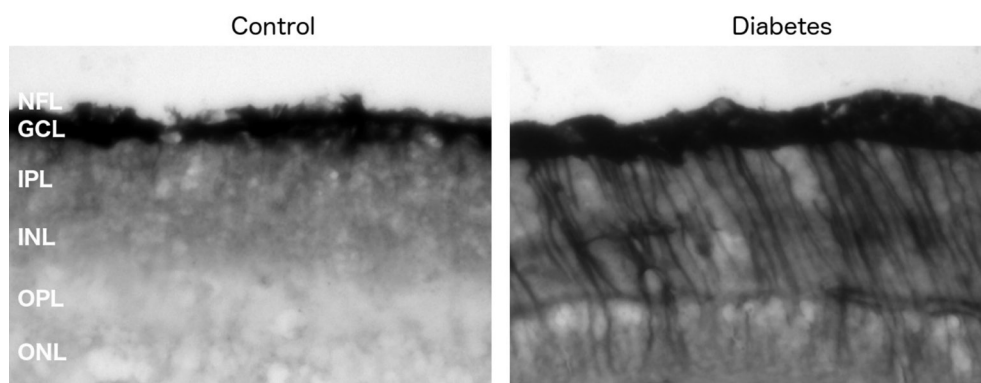
Immunohistochemistry, however, detected a change in distribution of PSA-NCAM in the diabetic retina. In control sections, PSA-NCAM immunopositive cells were observed mainly in the NFL, GCL, with some also present in the IPL close to the RGCs (Figure 3). Much lower PSA-NCAM

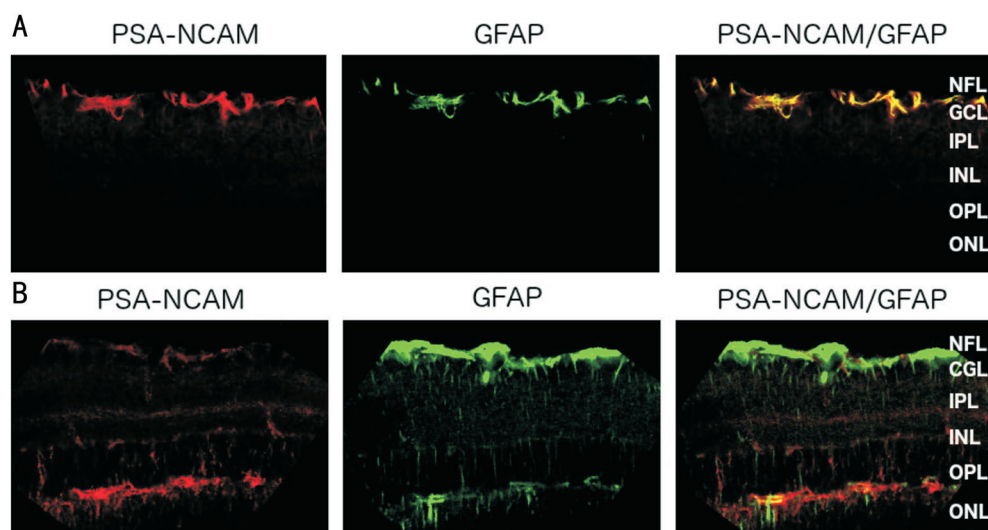**Table 1 Effect of diabetes on RGC and microglial cell densities**

Cell type	Cell density (cells/mm^2)		Change (%)
	Control	DR	
RGCs	3252±80	2637±101[a]	-19
Microglial cells	76±4	175±7[a]	+60

The data are expressed as the mean±SEM. [a]$P<0.0022$ (Mann-Whitney U test). RGCs: Retinal ganglion cells; DR: Diabetic retinopathy.

immunoreactivity was seen in the INL, OPL, and ONL of control retina (Figure 3). In contrast, in diabetic retina, a strong reduction in PSA-NCAM immunoreactivity (approximately 2.2-fold) was observed in the NFL and GCL where RGCs are located; however, enhanced PSA-NCAM immunoreactivity was observed in IPL, INL (approximately 1.3-fold) and especially the OPL, and ONL (about 2.3-fold), where processes and soma of Müller cells extend (Figure 3).

Figure 4 Representative microphotographs of GFAP immunoreactivity in retinal sections of control and diabetic mice Magnification ×200. NFL: Nerve fiber layer; GCL: Ganglion cell layer; IPL: Inner plexiform layer, INL: Inner nuclear layer; OPL: Outer plexiform layer; ONL: Outer nuclear layer.

Figure 5 Laser scanning images of sections double-labelled for PSA-NCAM (red) and GFAP (green) of control (A) and diabetic mice (B) Magnification ×400. NFL: Nerve fiber layer; GCL: Ganglion cell layer; IPL: Inner plexiform layer, INL: Inner nuclear layer; OPL: Outer plexiform layer; ONL: Outer nuclear layer.
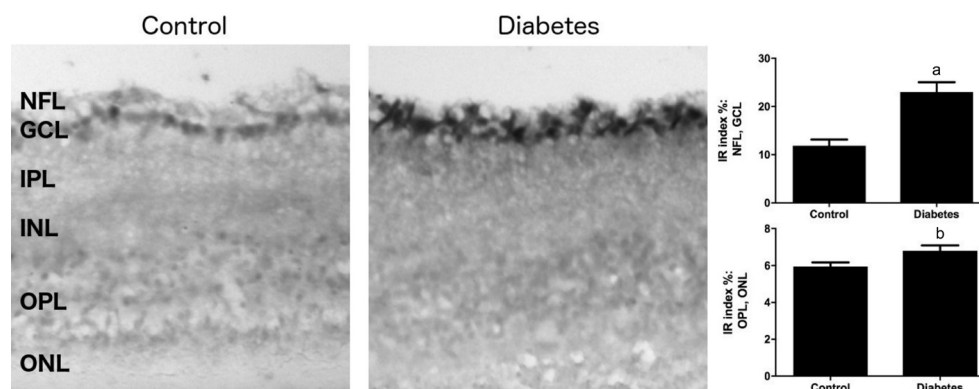
Changes in Glial Fibrillary Acidic Protein in the Retina of Diabetic Mice The distribution of GFAP was also changed in the diabetic retina. GFAP-positive immunostaining was confined to astrocytes and Müller cells, primarily in the NFL, and GCL of both control and diabetic retinas (Figure 4). In addition, in diabetic retinas, GFAP immunoreactivity was also strongly enhanced in the IPL, INL, OPL, and ONL (Figure 4). In control retinas, GFAP immunopositive filaments were mostly located in the endfeet of Müller cells and in adjoining internal stem processes. In contrast, in diabetic mice, GFAP-positive immunostaining in Müller cells was evident in the body, as well as along both inner and outer stem processes and their branches. GFAP levels were increased by approximately 2.0-fold in the retina of diabetic mice compared with control retinas (Figure 2B).

Co-localization studies of PSA-NCAM with GFAP demonstrated strong co-localization in control retina in the NFL and GCL. In contrast, in diabetic retina, PSA-NCAM was co-localized with GFAP primarily in the OPL and ONL (Figure 5).

Changes in the Levels of Matrix Metalloproteinase-9 in the Retina of Diabetic Mice It is well documented that DR is associated with the activation of metalloproteinases[33-35]. Previous studies have demonstrated that a reduction in PSA-NCAM levels in neuronal cells might be due to the activation of MMP-9, which induces shedding of extracellular PSA-NCAM[26]. We therefore measured MMP-9 levels in the retinas of the diabetic mice. Immunohistochemical staining revealed a prominent enhancement of MMP-9 (approximately 1.9-fold) in the NFL and GCL of diabetic retina compared with controls (Figure 6). In contrast, in IPL, INL, OPL, and ONL of diabetic retinas, MMP-9 levels were increased compared with controls albeit to a much lower extent (Figure 6).

DISCUSSION

STZ is known as a compound with preferential toxicity toward pancreatic β-cells. It is commonly used for the induction of diabetes in mice[3,27,36]. In our experiments, two consecutive doses (90 mg/kg) of STZ administered over 24-hour intervals induced diabetes in mice on day 7 after the last administration

Figure 6 Representative microphotographs of MMP-9 immunoreactivity in retinal sections of control and diabetic mice Magnification ×200. IR: Immunoreactivity; NFL: Nerve fiber layer; GCL: Ganglion cell layer; IPL: Inner plexiform layer; INL: Inner nuclear layer; OPL: Outer plexiform layer; ONL: Outer nuclear layer. The data are expressed as the mean±SEM. [a]$P<0.005$; [b]$P<0.01$ (Mann-Whitney U test).

as shown by the increased blood glucose levels and reduced body weight at this time point. At 2mo after STZ administration, the animals demonstrated increased density and hypertrophy of microglial cells, decreased density of RGCs, and reactive gliosis of Müller cells. Several authors have stated that these signs suggest the development of DR[11,37-38].

Immunohistochemical analysis of PSA-NCAM expression demonstrated a dramatic change in PSA-NCAM distribution in the diabetic retina. In diabetic retinas, PSA-NCAM signal is remarkably decreased in the NFL, GCL and strongly enhanced in the OPL, and ONL, whereas in control retina, prominent PSA-NCAM immunoreactivity was found in the NFL and GCL. In control retinas, PSA-NCAM is expressed in the endfeet of the inner stem processes of Müller cells and in the astrocytes, which are in close contact with RGCs in NFL, and GCL. In contrast, in the diabetic retina, PSA-NCAM is located in the Müller cell bodies (INL) and in inner and outer stem processes and their side branches (primarily the OPL and ONL).

The reduction of PSA-NCAM in GCL is associated with a decrease in RGC density in the diabetic retina. It was shown previously that PSA-NCAM supports RGC survival after optic nerve transection or after RGC injury[24,18].

We therefore propose that the reduced PSA-NCAM level in NFL and GCL is at least in part responsible for the loss of RGCs in the diabetic retina. This proposal is supported by the data clearly demonstrating the supportive roles of PSA-NCAM for the survival on neuronal and retinal cells[18,39]. The mechanisms by which PSA-NCAM promotes the survival of RGCs remain obscure. Some findings suggest that PSA-NCAM facilitates the brain derived neurotrophic factor (BDNF)-mediated phosphorylation of its receptor, TrkB, which promotes the neuronal survival[39]. BDNF and TrkB are abundantly present in the retina and may have a neuroprotective effect on RGC[40-42]. Also, increased p75 signalling after PSA removal might enhance neurons death[43]. The reason why PSA-NCAM is reduced in the NFL and GCL is not clearly understood. Previous studies have demonstrated

that MMPs might play a role in the regulation of PSA-NCAM levels[44-45]. A recent study from our laboratory has demonstrated that MMP-9 can induce degradation of PSA-NCAM[26].

Our study demonstrated an approximate 1.9-fold increase in MMP-9 expression in the NFL and GCL in diabetic retinas compared with controls and this might explain the observed reduction of PSA-NCAM in these retinal layers. Previous studies also have demonstrated MMP-9 upregulation in the diabetic retina[46-47]. It is proposed that MMP-9 is responsible for the degradation of PSA-NCAM in the NFL and GCL of diabetic retina. It was previously shown that intravitreal injection of MMP-9 inhibitor increases survival of RGC after retinal injury[48]. It should be noted, however, that a small but significant increase in MMP-9 levels was also observed in the other layers of the diabetic retina but it seems that this slight elevation cannot substantially impact PSA-NCAM shedding. The elevation of MMP-9 is most likely due to tissue inflammation, which accompanied DR. Furthermore, MMP-9 participates in angiogenesis by promoting endothelial cell migration, tubule formation, degradation of extracellular matrix and destruction of blood-retinal barrier[33-35,49]. Moreover, some evidence points to the fact that MMP-9 levels are higher in the vitreous humour in DR[34,50], which may additionally promote PSA-NCAM as well as NCAM cleavage in the inner part of the retina. It has been demonstrated also that PSA-NCAM is cleaved extracellularly by ADAM family metalloprotease[51-52]. We do not exclude that ADAM metalloproteases are also involved in the shedding of PSA-NCAM in the inner part of diabetic retina.

It is documented that diabetic hyperglycaemia causes hypoxia[53] and inflammation, which in turn induces proliferation of the processes of the Müller cells containing PSA-NCAM and GFAP. The role of an increase in PSA-NCAM in the IPL, INL and the OPL, and ONL of the diabetic retina is not clear but some evidence suggests that PSA-NCAM is involved in neovascularization in hypoxia-induced retinopathy[54].

PSA-NCAM may also act as a guide for proliferative and migratory Müller cell processes in DR[55].

In conclusion, our findings demonstrate that a decrease in PSA-NCAM levels in the NFL and GCL is associated with lower density of RGCs in diabetic retinas. A large increase in MMP-9 levels in NFL and GCL cause PSA-NCAM cleavage in the inner part of the retina. The causal relationship between PSA-NCAM and RGC survival, however, remains unclear. Currently the studies aiming at elucidation the roles of MMPs in the shedding of PSA-NCAM and the mechanisms by which PSA-NCAM regulates RGC survival are in progress in our laboratory.

REFERENCES
1 Olivares AM, Althoff K, Chen GF, Wu S, Morrisson MA, DeAngelis MM, Haider N. Animal models of diabetic retinopathy. *Curr Diab Rep* 2017;17(10):93.

2 Cui J, Gong R, Hu S, Cai L, Chen L. Gambogic acid ameliorates diabetes-induced proliferative retinopathy through inhibition of the HIF-1a/VEGF expression via targeting PI3K/AKT pathway. *Life Sci* 2018;192:293-303.

3 Kim SJ, Kim H, Park J, Chung I, Kwon HM, Choi WS, Yoo JM. Tonicity response element binding protein associated with neuronal cell death in the experimental diabetic retinopathy. *Int J Ophthalmol* 2014;7(6):935-940.

4 Mei X, Zhou L, Zhang T, Lu B, Sheng Y, Ji L. Chlorogenic acid attenuates diabetic retinopathy by reducing VEGF expression and inhibiting VEGF-mediated retinal neoangiogenesis. *Vascul Pharmacol* 2018;101:29-37.

5 Tonade D, Liu H, Palczewski K, Kern TS. Photoreceptor cells produce inflammatory products that contribute to retinal vascular permeability in a mouse model of diabetes. *Diabetilogia* 2017;60(10):2111-2120.

6 Gilbert ER, Fu Z, Liu D. Development of a nongenetic mouse model of type 2 diabetes. *Exp Diabetes Res* 2011;2011:416254.

7 Tang F, Pacheco MTF, Chen P, Liang D, Li W. Secretogranin III promotes angiogenesis through MEK/ERK signalling pathway. *Biochem Biophys Res Commun* 2018;495(1):781-786.

8 Sohn EH, Dijk HW, Jiao C, Kok PH, Jeong W, Demirkaya N, Garmager A, Wit F, Kucukevcilioglu M, Velthoven ME, DeVries JH, Mullins RF, Kuehn MH, Schlingemann RO, Sonka M, Verbraak FD, Abramoff MD. Retinal neurodegeneration may precede microvascular changes characteristic of diabetic retinopathy in diabetes mellitus. *Proc Natl Acad Sci U S A* 2016;1113(19):E2655-E2664.

9 Zhang J, Wu Y, Jin Y, Ji F, Sinclair SH, Luo Y, Xu G, Lu L, Dai W, Yanoff M, Li W, Xu GT. Injection of erythropoietin protects both retinal vascular and neuronal cells in early diabetes. *Invest Ophthalmol Vis Sci* 2008;49(2):732-742.

10 Jung KI, Kim JH, Park HY, Park CK. Neuroprotective effects of cilostazol on retinal ganglion cell damage in diabetic rats. *J Pharmacol Exp Ther* 2013;345(3):457-463.

11 Fernandez-Bueno I, Jones R, Soriano-Romani L, Lopez-Garcia A, Galvin O, Cheetham S, Diebold Y. Histologic characterization of retina neuroglia modifications in diabetic zucker diabetic fatty rats. *Invest Ophthalmol Vis Sci* 2017;58(11):4925-4933.

12 Feit-Leichman RA, Kinouchi R, Takeda M, Fan Z, Mohr S, Kern TS, Chen DF. Vascular damage in a mouse model of diabetic retinopathy: relation to neuronal and glial changes. *Invest Ophthalmol Vis Sci* 2005;46(11):4281-4287.

13 Kern TS, Barber AJ. Retinal ganglion cells in diabetes. *J Physiol (Lond)* 2008;586(18):4401-4408.

14 Rothbard JB, Brackenbury R, Cunningham BA, Edelman GM. Differences in the carbohydrate structures of neural cell-adhesion molecules from adult and embryonic chicken brains. *J Biol Chem* 1982;257(18):11064-11069.

15 Seki T, Arai Y. Distribution and possible roles of the highly polysialylated neural cell adhesion molecule (NCAM-H) in the developing and adult central nervous system. *Neurosci Res* 1993;17(4):265-290.

16 Eckhardt M, Bukalo O, Chazal G, Wang L, Goridis C, Schachner M, Gerardy-Schahn R, Cremer H, Dityatev A. Mice deficient in the polysialyltransferase ST8SiaIV/PST-1 allow discrimination of the roles of neural cell adhesion molecule protein and polysialic acid in neural development and synaptic plasticity. *J Neurosci* 2000;20(14):5234-5244.

17 Bartsch U, Kirchhoff F, Schachner M. Highly sialylated N-CAM is expressed in adult mouse optic nerve and retina. *J Neurocytol* 1990;19(4): 550-565.

18 Murphy JA, Hartwick AT, Rutishauser U, Clarke DB. Endogenous polysialylated neural cell adhesion molecule enhances the survival of retinal ganglion cells. *Invest Ophthalmol Vis Sci* 2009;20(2):861-869.

19 Kobayashi S, Vidal I, Pena JD, Hernandez MR. Expression of neural cell adhesion molecule (NCAM) characterizes a subpopulation of type 1 astrocytes in human optic nerve head. *Glia* 1997;20(3):262-273.

20 McKay BS, Irving PE, Skumatz CM, Burke JM. Cell-cell adhesion molecules and the development of an epithelial phenotype in cultured human retinal pigment epithelial cells. *Exp Eye Res* 1997;65(5):661-671.

21 Chan-Ling T. Glial, neuronal and vascular interactions in the mammalian retina. *Prog Ret Eye Res* 1994;13(1):357-389.

22 Stone J, Dreher Z. Relationship between astrocytes, ganglion cells and vasculature of the retina. *J Comp Neurol* 1987;255:35-49.

23 Stone J, Makarov F, Holländer H. The glial ensheathment of the soma and axon hillock of retinal ganglion cells. *Vis Neurosci* 1995;12(2):273-279.

24 Lobanovskaya N, Zharkovsky T, Jaako K, Jürgenson M, Aonurm-Helm A, Zharkovsky A. PSA modification of NCAM supports the survival of injured retinal ganglion cells in adulthood. *Brain Res* 2015;1625:9-17.

25 Murphy JA, Franklin TB, Rafuse VF, Clarke DB. The neural cell adhesion molecule is necessary for normal adult retinal ganglion cell number and survival. *Mol Cell Neurosci* 2007;36(2):280-292.

26 Jaako K, Waniek A, Parik K, *et al*. Prolyl endopeptidase is involved in the degradation of neural cell adhesion molecules in vitro. *J Cell Sci* 2016;129(20):3792-3802.

27 Devi L, Alldred MJ, Ginsbrg SD, Ohno M. Mechanisms underlying insulin deficiency-induced acceleration of β-amyloidosis in a mouse model of Alzheimer's disease. *PLoS One* 2012;7(3):e32792.

28 Nadal-Nikolas FM, Jimenes-Lopez M, Sobrado-Calvo P, Nieto-Lopez L, Canovas-Martinez I, Salinas-Navarro M, Vidal-Sanz M, Agudo M. Brn3a as a marker of retinal ganglion cells: qualitative and quantitative time course studies in naïve and optic nerve-injured retinas. *Invest Ophthalmol Vis Sci* 2009;50(8):3860-3868.

29 Quina LA, Pak W, Lanier J, Banwait P, Gratwick K, Liu Y, Velasquez T, O'Leary DD, Goulding M, Turner EE. Brn3a-expressing retinal ganglion cells project specifically to thalamocortical and collicular visual pathways. *J Neurosci* 2005;25(50):11595-11604.

30 Ito D, Imai Y, Ohsawa K, Nakajima K, Fukuuch Y, Kohsaka S. Microglia-specific localisation of a novel calcium binding protein, Iba1. *Brain Res Mol Brain Res* 1998;57(1):1-9.

31 Goodchild AK, Martin PR. The distribution of calcium-binding proteins in the lateral geniculate nucleus and visual cortex of a New World monkey, the marmoset, Callithrix jacchus. *Vis Neurosci* 1998;15(4):625-642.

32 Sia Y, Bourne JA. The rat temporal association cortical area 2 (Te2) comprises two subdivisions that are visually responsive and develop independently. *Neuroscience* 2008;156(1):118-128.

33 Di Y, Nie QZ, Chen XL. Matrix metalloproteinase-9 and vascular endothelial growth factor expression change in experimental retinal neovascularization. *Int J Ophthalmol* 2016;9(6):804-808.

34 Mohammad G, Siddiquei MM. Role of matrix metalloproteinase-2 and -9 in the development of diabetic retinopathy. *J Ocul Biol Dis Infor* 2012;5(1):1-8.

35 Salzmann J, Limb GA, Khaw PT, Gregor ZJ, Webster L, Chignell AH, Charteris DG. Matrix metalloproteinases and their natural inhibitors in fibrovascular membranes of proliferativediabetic retinopathy. *Br J Ophthalmol* 2000;84(10):1091-1096.

36 Graham ML, Janecek JL, Kittredge JA, Hering BJ, Schuurman HJ. The streptozotocin-induced diabetic nude mouse model: differences between animals from different sources. *Comp Med* 2011;61(4):356-360.

37 Kern TS, Barber AJ. Retinal ganglion cells in diabetes. *J Physiol (Lond)* 2008;586(18):4401-4408.

38 Zeng XX, Ng YK, Ling EA. Neuronal and microglial response in the retina of streptozotocin-induced diabetic rats. *Vis Neurosci* 2000;17(3):463-471.

39 Vutskits L, Djebbara-Hannas Z, Zhang H, Paccaud JP, Durbec P, Rougon G, Muller D, Kiss JZ. PSA-NCAM modulates BDNF-dependent survival and differentiation of cortical neurons. *Eur J Neurosci* 2001;13(7):1391-1402.

40 Vecino E, Garcia-Grespo D, Garcia-Grespo M, Martinez-Milan L, Sharma SC, Carrascal E. Rat retinal ganglion cells co-express brain derived neurotrophic factor (BDNF) and its receptor TrkB. *Vision Res* 2002;42(2):151-157.

41 Domenici L, Origlia N, Falsini B, Cerri E, Barloscio D, Fabiani C, Sanso M, Giovanni L. Rescue of retinal function by BDNF in mouse model of glaucoma. *PLoS One* 2014;9(12):e115579.

42 Chen H, Weber AJ. BDNF enhances retinal ganglion cell survival in cats with optic nerve damge. *Invest Ophthalmol Vis Sci* 2001;42(5):966-974.

43 Gascon E, Vutskis L, Jenny B, Durbec P, Kiss JZ. PSA-NCAM in postnatally generated immature neurons of the olfactory bulb: a crucial role in regulating p75 expression and cell survival. *Development* 2007;134(6):1181-1190.

44 Hinkle CL, Diestel S, Lieberman J, Maness PF. Metalloprotease-induced ectodomain shedding of neural cell adhesion molecule (NCAM). *J Neurobiol* 2006;66(12):1378-1395.

45 Hübschmann MV, Skladchikova G, Bock E, Berezin V. Neural cell adhesion molecule function is regulated by metalloproteinase-mediated ectodomain release. *J Neurosci Res* 2005;80(6):826-837.

46 Beranek M, Kolar P, Tschoplova S, Kankova K, Vasku A. Genetic variations and plasma levels of gelatinase A (matrix metalloproteinase-2) and gelatinase B (matrix metalloproteinase-9) in proliferative diabetic retinopathy. *Mol Vis* 2008;14:1114-1121.

47 Das A, McGuire PG, Eriqat C, Ober RR, DeJuan E Jr, Williams GA, McLamore A, Biswas J, Johnson DW. Human diabetic neovascular membranes contain high levels of urokinase and metalloproteinase enzymes. *Invest Ophthalmol Vis Sci* 1999;40(3):809-813.

48 Zhang X, Cheng M, Chintala SK. Kainic acid-mediated upregulation of matrix metalloproteinase-9 promotes retinal degeneration. *Invest Ophthalmol Vis Sci* 2004;45(7):2374-2383.

49 Kowluru, RA. Role of matrix metalloproteinase-9 in the development of diabetic retinopathy and its regulation by H-Ras. *Invest Ophthalmol Vis Sci* 2010;51(8):4320-4326.

50 Abu El-Asrar AM, Mohammed G, Nawaz MI, Siddiquei MM, Van den Eynde K, Mousa A, De Hertogh G, Opdenakker G. Relationship between vitreous levels of matrix metalloproteinase and vascular endothelial growth factor in proliferative diabetic retinopathy. *PLoS One* 2013;8(12):e85857.

51 Kalus I, Bormann U, Mzoughi M, Schachner M, Kleene R. Proteolytic cleavage of the neural cell adhesion molecule by ADAM17/TACE is involved in neurite outgrowth. *J Neurochem* 2006;98(1):78-88.

52 Brennaman LH, Moss ML, Maness PF. EphrinA/EphA-induced ectodomain shedding of neural cell adhesion molecule regulates growth cone repulsion through ADAM10 metalloprotease. *J Neurochem* 2014;128(2):267-279.

53 Schröder S, Palinski W, Schmid-Schönbein GW. Activated monocytes and granulocytes, capillary nonperfusion, and neovascularization in diabetic retinopathy. *Am J Pathol* 1991;139(1):81-100.

54 Håkansson J, Ståhlberg A, Wolfhrgen Sand F, Gerhardt H, Semb H. N-CAM exhibits a regulatory function in pathological angiogenesis in oxygen induced retinopathy. *PLoS One* 2011;6(10):e26026.

55 Burke JM, Smith JM. Retinal proliferation in response to vitreous hemoglobin or iron. *Invest Ophthalmol Vis Sci* 1981;20(5):582-592.